Strategies for Fast Control Speed and DC Drift Avoidance in Distributed $LiNbO_3$-Based PMD Compensators

Reinhold Noé, *Member, IEEE,* and David Sandel

***Abstract*—Cascaded mode converters on a birefringent X-cut Y-propagation $LiNbO_3$ chip are ideal "distributed" polarization-mode dispersion (PMD) compensators. Here, we show how the number of needed control variables can be minimized to permit fastest PMD compensation. Furthermore, a strategy is laid out which allows us to apply zero-mean control voltages for avoidance of the dc drift effect.**

***Index Terms*—DC drift, differential group delay (DGD) profile, $LiNbO_3$, polarization-mode dispersion compensator (PMDC).**

I. Introduction

POLARIZATION-MODE dispersion (PMD) [1] is a big obstacle for high-capacity long-haul optical communication systems, but can, in principle, be fully removed by an optical PMD compensator (PMDC). Each of its polarization transformers must be able to endlessly transform any input polarization into a principal state-of-polarization of the subsequent differential group delay (DGD) section [2].

A "distributed" PMDC with cascaded in-phase and quadrature mode converters in X-cut Y-propagation $LiNbO_3$ is best suited because of its ability to correct higher orders of PMD, and its fast electrooptic response [3], [4]. Waveguide nonuniformity can significantly decrease the conversion efficiency of long mode converters. Apart from improved fabrication, the only way to combat it is to subdivide the mode converters into fairly short sections. However, it has been argued that a large number of electrode voltages can not be controlled sufficiently fast. Here, we show that this is not true, that waveguide nonuniformity, highest mode conversion efficiency, and fastest control speed do not exclude each other.

Another potential problem is dc drift [5]: Charges generated by the pyroelectric effect are separated under the influence of a static external electric field, thereby weakening this field inside and near the waveguide. Ion migration in the buffer layer and/or conductivity disturbances of the crystal cause a similar effect. DC drift limits are not known or at least not specified for commercial $LiNbO_3$ polarization transformers. We show that distributed PMDCs can be driven by dc-free voltages, which avoids drift altogether.

Manuscript received February 25, 2003; revised August 1, 2003. This work was supported in part by Siemens ICN.

The authors are with the University of Paderborn, D-33098 Paderborn, Germany (e-mail: noe@upb.de).

Digital Object Identifier 10.1109/LPT.2004.824959

II. Reduced Number of Control Parameters Is Compatible With Nonuniform Waveguide

An in-phase and quadrature mode converter may be called a Soleil–Babinet analog [(SBA) φ, ψ] [2] because of the analogy to a Soleil–Babinet compensator. This retarder is described by a Jones matrix or a 3×3 rotation matrix (= Mueller submatrix), as shown in the equation at the bottom of the next page, respectively. A DGD τ is represented by a phase shifter [(PS) $-\omega\tau$] with Jones and rotation matrices

$$\begin{bmatrix} 1 & 0 \\ 0 & e^{j\omega\tau} \end{bmatrix} \quad \begin{bmatrix} 1 & 0 & 0 \\ 0 & \cos\omega\tau & \sin\omega\tau \\ 0 & -\sin\omega\tau & \cos\omega\tau \end{bmatrix}$$

respectively, where ω is the optical angular frequency. The whole distributed PMDC is approximately described by the Jones or rotation matrix product

$$\mathrm{PMDC} = \prod_{i=n}^{1} (\mathrm{PS}(-\omega\tau_i)\mathrm{SBA}(\varphi_i, \psi_i)). \tag{1}$$

The product must be executed from left to right with descending index i while the light passes the SBAs and PSs in ascending order i. A longitudinally variable pattern of in-phase voltages $V_{1,i}$ and quadrature voltages $V_{2,i}$ couples transverse electric (TE) and transverse magnetic (TM) modes. Using a constant G, we can write

$$\varphi_i e^{j\psi_i} = G(V_{1,i} + jV_{2,i}). \tag{2}$$

A pigtailed PMDC similar to that in [3] and [4] was electrooptically investigated. It had $n = 69$ pairs of in-phase and quadrature electrodes, each segment $i = 1 \ldots n$ being ~1.27 mm long. The total PMD was ~23 ps, which is good for 40-Gb/s PMD compensation. The PMDC was operated with a horizontal input polarization in the waveguide. A polarimeter was connected to the PMDC output. Consider the case when all voltages except those of segment i are zero. With PMDC given by its Jones or its rotation matrix, the output polarization state can be expressed by the Jones or normalized Stokes vector

$$\begin{bmatrix} \cos\varphi_i/2 \\ je^{-j(\psi_i+\zeta_i)}\sin\varphi_i/2 \end{bmatrix} = \mathrm{PMDC} \cdot \begin{bmatrix} 1 \\ 0 \end{bmatrix}$$
$$\begin{bmatrix} \cos\varphi_i \\ \sin(\psi_i+\zeta_i)\sin\varphi_i \\ -\cos(\psi_i+\zeta_i)\sin\varphi_i \end{bmatrix} = \mathrm{PMDC} \cdot \begin{bmatrix} 1 \\ 0 \\ 0 \end{bmatrix} \tag{3}$$

1041-1135/04$20.00 © 2004 IEEE

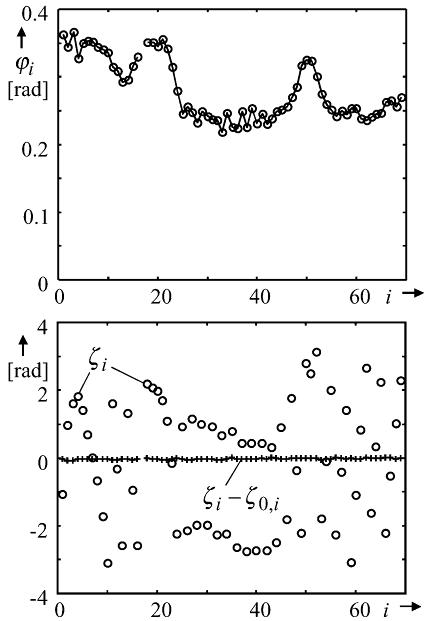

Fig. 1. Polarization change φ_i (left), and its orientation ζ_i (o) and orientation error $\zeta_i - \zeta_{0,i}(+$, solid line) for $V_{1,i} + jV_{2,i} = 20$ V (right). Point $i = 17$, where both electrodes had internal shorts to ground, is omitted.

respectively. Here, $\zeta_i = -\omega \sum_{k=i}^{n} \tau_k$ are phase shifts. If they are modulo 2π unequal then the waveguide is nonuniform. Four voltage pairs $V_{1,i} + jV_{2,i} = 20\text{V} \cdot \{1, j, -1, -j\}$ were applied sequentially to each of the electrodes in section i, and the output polarization state was measured. Equations (2) and (3) allowed us to determine φ_i and ζ_i. Performance was best at $\lambda = 1540$ nm, where φ_i varied somewhat as a function of i, but not too much (Fig. 1). However, ζ_i varied a lot. If a number of adjacent in-phase electrodes were connected in parallel, and likewise for quadrature electrodes, then a low mode conversion efficiency would result, especially for $i = 25 \ldots 45$ where adjacent ζ_i differ by about π.

There is a simple remedy: The voltage pairs $V_{1,i} + jV_{2,i}$ in (2) are not applied directly but are first multiplied by $e^{-j\zeta_{0,i}}$. This replaces $\psi_i + \zeta_i$ in (3) by $\psi_i + \zeta_i - \zeta_{0,i}$. The values $\zeta_{0,i}$ should be equal to ζ_i and must be measured once in factory for all i. We took the measured ζ_i values as the calibration set $\zeta_{0,i}$, and repeated the measurement to obtain new ζ_i values and test stability, under temperature control. Fig. 1 shows the resulting orientation error $\zeta_i - \zeta_{0,i}$. It ranged from -0.08 to $+0.01$ rad and may be partly due to multipath reflections at the straight chip endfaces. Now, the effects of any set of segments can be combined because the quantity $\varphi_i e^{j(\psi_i + \zeta_i)} \approx \varphi_i e^{j(\psi_i + \zeta_{0,i})}$ has become user-accessible.

In PMD compensation algorithms, it is common to dither various electrode voltages, one at a time, and to optimize them by a multidimensional gradient search using one or more control criteria. For a maximum voltage of 55 V (=10 V/μm), a waveguide length of $\sim 4 \ldots 6$ mm will be needed for full mode conversion, and it is, therefore, possible to reduce the number of control variables below 2 n. A straightforward approach is to specify, say, 4 "discrete" polarization transformers at $0, L/4, L/2$ and $3L/4$, where L is the chip length. Due to the previous calibration process, just two control variables are required per polarization transformation, which is the physically necessary minimum. Such a PMDC needs ≤ 48 voltages but just eight control variables, and is four times more powerful than a PMDC featuring one commercial X-cut Z-propagation $LiNbO_3$ device, which requires up to 16 control variables for its eight waveplates.

An alternative approach, which may permit highest PMDC performance, employs a number of spatial Fourier coefficients $F_k = n^{-1} \sum \varphi_i e^{j(\psi_i + \zeta_{0,i})} e^{-j2\pi ik/n}$ as control variables. The required inverse Fourier transform and multiplication can be implemented in a field programmable gate array for fast execution

$$V_{1,i} + jV_{2,i} = G^{-1} e^{-j\zeta_{0,i}} \sum F_k e^{j2\pi ik/n}.$$

The PMD vector Ω has a length equal to the DGD and points in the direction of a principal state-of-polarization in the three-dimensional normalized Stokes space. If n DGD sections are cascaded, the overall PMD vector is given the sum $\Omega = \sum_{i=1}^{n} \Omega_i$ of individual PMD vectors $\Omega_i = \mathbf{R}_{<i}^{-1} \Omega_{\text{local},i}$. The Ω_i are referred to the input of the whole cascade, whereas, $\Omega_{\text{local},i}$ are the local individual PMD vectors. $\mathbf{R}_{<i}$ is the 3×3 rotation matrix representing all DGD sections (PSs) and SBAs which precede the DGD section i. Plotting the sequence of Ω_i in such a way that the tail of Ω_{i+1} starts from the head of Ω_i results in a DGD profile [2], [6]. Its endpoint is given by $\mathbf{\Omega}$. For a distributed PMDC, the DGD profile is a straight rod as long as no voltages are applied. The Fourier coefficient F_0 causes a bend or loop, and F_k with $k \neq 0$ a spiral of the DGD profile. The coefficiencts permit a precise control of the DGD profile shape. Some 38 control variables or so (real and imaginary parts of $F_k, k = -9, -8, \ldots, 9$) may be sufficient for a 96-mm-long chip. If the center of gravity of the coefficient spectrum, root-mean-square-averaged over extended times, is not near $k = 0$, there may be a static phase mismatch. To overcome it, one may correct the chip temperature: A temperature change by $k\cdot$ ($\pm$0.44 K) will translate the center of gravity from k to zero for a 96-mm-long chip. The sign depends on the definition of in-phase versus quadrature.

$$\begin{bmatrix} \cos\varphi/2 & je^{j\psi}\sin\varphi/2 \\ je^{-j\psi}\sin\varphi/2 & \cos\varphi/2 \end{bmatrix}$$

$$\begin{bmatrix} \cos\varphi & -\sin\psi\sin\varphi & \cos\psi\sin\varphi \\ \sin\psi\sin\varphi & \cos^2\psi + \sin^2\psi\cos\varphi & \cos\psi\sin\psi(1-\cos\varphi) \\ -\cos\psi\sin\varphi & \cos\psi\sin\psi(1-\cos\varphi) & \sin^2\psi + \cos^2\psi\cos\varphi \end{bmatrix}$$

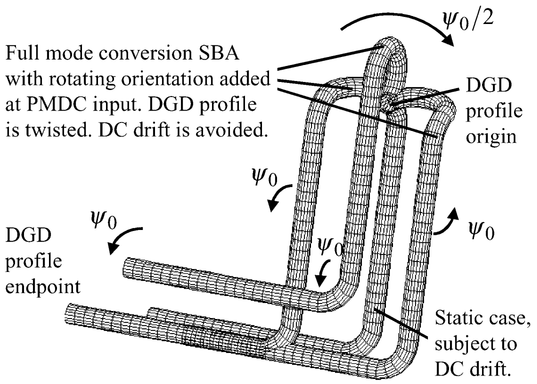

Fig. 2. Mechanical analog with flexible but torsion-stiff rod: DGD profiles of a PMDC (static case) and a dc drift-free PMDC (three other instantiations).

III. Zero-Mean Voltages for Suppression of DC Drift Effects

Fig. 2 shows DGD profiles of two distributed PMDCs. When bending radii are short enough, these DGD profiles are equivalent. In one of the PMDCs (static case), dc drift may cause the joints to straighten out instead of staying bent, thereby distorting the DGD profile or requiring higher and higher voltages. In the other PMDC, an SBA has been added at the input. That SBA performs a full mode conversion (U turn) under a suitable, slowly, and linearly time-variable orientation angle $\psi_1 + \psi_0/2$, with $\psi_0 = 2\pi ft$. The TE–TM phase difference at its output is shifted by ψ_0. The frequency f may be in the microhertz–hertz range. As a consequence, all following SBAs must rotate their orientations by ψ_0 to approximately maintain the overall DGD profile shape. Mathematically speaking, the expression (1) is identical with

$$\begin{aligned}\mathrm{PMDC} = {} & \mathrm{SBA}(\pi, \psi_0/2)\mathrm{SBA}(\pi, \pi + \psi_0)\\ & \cdot \prod_{i=n}^{2} (\mathrm{PS}(-\omega\tau_i)\mathrm{SBA}(\varphi_i, \psi_i + \psi_0))\\ & \cdot \mathrm{PS}(-\omega\tau_1)\mathrm{SBA}(\pi - \varphi_1, \psi_1 + \pi + \psi_0)\\ & \cdot \mathrm{SBA}(\pi, \psi_1 + \psi_0/2). \end{aligned} \tag{4}$$

The $\mathrm{SBA}(\pi, \psi_0/2)\mathrm{SBA}(\pi, \pi + \psi_0)$ at the end of the PMDC may be left out if, as usual, a constant output polarization is not needed. That case, where a full mode conversion SBA is added only at the PMDC input, is illustrated in Fig. 2 for three different ψ_0. All driving voltages are pure ac voltages. DC drift is thereby avoided, at the cost of losing direct control over $1 \ldots 1.5$ ps of DGD in a small input portion of the PMDC. Errors which may occur due to imperfect PMDC characterization can be corrected by slight changes of the PMD profile bends. For this purpose, the control algorithm must simultaneously optimize all φ_i, ψ_i in (4) or all F_k, while $\psi_0 = 2\pi ft$ is being incremented automatically at a sufficiently low speed.

IV. Conclusion

Solutions for the most challenging practical problems of distributed PMDCs in X-cut Y-propagation $LiNbO_3$ have been pointed out: Waveguide nonuniformity effects can be calibrated out, and a limited number of control variables provides an efficient control even though there may be many electrodes. In particular, two control variables per polarization transformation are sufficient, which is the physically necessary minimum. DC drift, which is a severe limiting factor in X-cut Z-propagation $LiNbO_3$ polarization transformers, can be avoided altogether in distributed PMDCs because they can be driven by pure ac voltages.

Acknowledgment

The authors would like to thank R. Ricken, H. Herrmann, and W. Sohler of the University of Paderborn for device fabrication.

References

[1] C. D. Poole and R. E. Wagner, "Phenomenological approach to polarization dispersion in long single-mode fibers," *Electron. Lett.*, vol. 22, pp. 1029–1030, 1986.
[2] R. Noé *et al.*, "Polarization mode dispersion compensation at 10, 20, and 40 Gb/s with various optical equalizers," *J. Lightwave Technol.*, vol. 17, pp. 1602–1616, Sept. 1999.
[3] R. Noé *et al.*, "Integrated optical $LiNbO_3$ distributed polarization mode dispersion equalizer in 20 Gbit/s transmission system," *Electron. Lett.*, vol. 35, no. 8, pp. 652–654, 1999.
[4] D. Sandel *et al.*, "Integrated-optical polarization mode dispersion compensation for 6-ps, 40-Gb/s pulses," in *Proc. Eur. Conf. Integrated Optics (ECIO'99)*, Turin, Italy, Apr. 14–16, 1999, pp. 17–19.
[5] J. Nayyer *et al.*, "Fabrication of high-speed asymmetric Ti:$LiNbO_3$ Mach-Zehnder optical modulators with improved thermal-drift characteristics," in *Proc. Int. Conf. on Integrated Optics and Optical Fibre Communications (IOOC'95)*, vol. 2, Hong Kong, June, 26–30 1995, Paper WD1-5.
[6] R. Noé, "Combatting and equalizing the effects of PMD in 40 Gb/s systems and beyond," in *Proc. Eur. Conf. Optical Communications (ECOC 2002)*, vol. II, Copenhagen, Denmark, 2002, Paper T4.